Voprosy Onkologii = Problems in Oncology. 2026. Vol. 72, No 2
UDC 616-006-018:612.017.1
DOI 10.37469/0507-3758-2026-2-OF-2501

© *Tatyana L. Nekhaeva, Anna B. Danilova, Natalya A. Efremova, Aleksei O. Danilov, Ekaterina S. Zuy, Irina A. Baldueva*

The Prognostic Role of Cellular Models in Evaluating the Efficacy of Dendritic Cell Vaccines

N.N. Petrov National Medical Research Center of Oncology, St. Petersburg, the Russian Federation

Introduction. Anticancer vaccines based on activated dendritic cells (DCs) are of significant interest. Constructing and utilizing cellular models that reproduce immunological responses for monitoring such therapy and predicting disease outcomes is a promising approach.

Aim. To develop autologous cellular models that reproduce *in vitro* activation of antitumor mechanisms following exposure to a DC vaccine and to study their prognostic value during treatment.

Materials and Methods. Biological material was obtained from 11 patients (7 with skin melanoma, 4 with soft tissue or osteogenic sarcomas (STS/OS) treated with the autologous CaTeVac vaccine in N.N. Petrov National Medical Research Center of Oncology. Cellular models were created using cultures of patient-derived tumor cells and T-lymphocytes activated via coculture with vaccine DCs. The models were analyzed using flow cytometry, enzyme-linked immunosorbent assay (ELISA), and assessment of tumor cell proliferation potential.

Results. Generation of activated T-lymphocytes in response to vaccine DC stimulation was observed in 90.9 **%** of patients prior to treatment. The modeled interaction between T-lymphocytes and autologous tumor cells reproduced the clinical response in in 8 out of 11 (72.7 **%**) of cases. Inverse correlations were found between the levels of MICA and $TGF\beta_1$ secreted by tumor cells and the cell lysis ratio (rho = –0.792, p = 0.001 and rho = –0.472, p = 0.048, respectively), and between relative content of proliferating $CD3^+CFSE^+$ lymphocytes and plasma concentrations of IL-10 (rho = –0.579, p = 0.019) and $TGF\beta_1$ (rho = –0.512, p = 0.043) in patients' peripheral blood before treatment. During the formation of a proliferating $CD3^+$ cell clone, an increase in the subset of terminally differentiated lymphocytes (TEMRA) $CD4^+$ (p = 0.018) and CD8+ (p = 0.048) was observed in patients with a sufficient effect (SE) before treatment compared to those with an insufficient effect (IE). After 2–6 cycles of DCV, SE patients experienced a significant increase in the number of CD8+ effector memory cells ($CD8^+$Tem) (p = 0.036) and TEMRA $CD8^+$ lymphocytes producing granzyme B (TEMRA GrB^+CD8^+) (p = 0.025).

Conclusion. The cytotoxic properties of antigen-specific T-lymphocytes induced by mature DCs vary between patients and correlate with the clinical disease presentation and therapy response. This supports the use of 2D and 3D cellular modeling as an *in vitro* method for predicting and monitoring the efficacy of dendritic cell-based immunotherapy.

Keywords: dendritic cell vaccines; cellular models; melanoma; sarcoma; cytotoxic lymphocytes

For Citation: Tatyana L. Nekhaeva, Anna B. Danilova, Natalya A. Efremova, Aleksei O. Danilov, Ekaterina S. Zuy, Irina A. Baldueva. The prognostic role of cellular models in evaluating the efficacy of dendritic cell vaccines. *Voprosy Onkologii = Problems in Oncology*. 2026; 72(2): 00-00.-DOI: 10.37469/0507-3758-2026-2-OF-2501

✉ Contacts: Nekhaeva Tatyana L., nehaevat151274@mail.ru

Introduction

Among immunotherapeutic approaches currently under development, considerable attention is focused on tumor vaccines based on activated dendritic cells (DCs). The principal mechanism of these vaccines involves immunizing patients with immunogenic peptides derived from tumor-associated antigens, thereby inducing a polyvalent adaptive immune response directed specifically against malignant tumor cells [1].

DCs, often referred to as "nature's adjuvants," are professional antigen-presenting cells that play a critical role in stimulating adaptive immune responses by providing three essential signals required for lymphocyte activation. First, DCs process both intracellular and extracellular antigens and present antigen-derived peptides on major histocompatibility complex (MHC) class I or II molecules to $CD8^+$ and $CD4^+$ T lymphocytes, respectively. Second, DCs deliver crucial co-stimulatory signals to lymphocytes, predominantly mediated by the CD80/CD86 : CD28 interaction. Finally, DCs secrete polarizing cytokines such as interleukin-12 (IL-12), which stimulate the effector functions of lymphocytes. Through their interaction with DCs, naïve T cells differentiate into effector T cells, culminating in the generation of tumor-specific cellular and humoral immune responses. Consequently, DCs, as key mediators of the immune response, represent a highly promising foundation for a multitude of cancer vaccine strategies [2].

DCs also possess the ability to coordinate not only adaptive but also innate immunity. Within the innate immune system, DCs secrete protective cytokines such as IL-6 and IL-12, and growth factors, in response to "danger" signals, modulating ongoing immune reactions. Furthermore, DCs directly interact with innate immune cells, including natural killer cells, macrophages, and mast cells, thereby orchestrating a robust and comprehensive immune response [3].

Evidence indicates that cancer patients exhibit both quantitative and functional deficiencies in DC populations, with the reduction more pronounced in metastatic compared to early-stage primary tumors [4]. The immunosuppressive microenvironment established by malignant cells impedes DC maturation and function, resulting in deficient tumor-specific immune responses [5]. Moreover, deficient immunogenicity in so-called "cold" tumors is frequently attributed either to the absence of T cell infiltration or to their dysfunctional/exhausted status. These defects within the cancer-immunity cycle can be addressed through dendritic cell vaccines (DCVs).

The most commonly employed method of DCV production is the sensitization of DCs with tumor antigens obtained from tumor cell lysates. Immature DCs, loaded with patient-derived tumor antigens, subsequently differentiate into mature DCs, which, once antigen-equipped, are reintroduced into patients to potentiate antitumor immune activation *in vivo* [6].

A critical aspect in achieving DCV efficacy lies in the identification and investigation of factors that allow prediction of disease outcome and selection of cancer patients most likely to respond favorably to treatment. The design and application of cellular models that replicate the extent of restoration of immune responses targeting the recognition and elimination of patient tumor cells following DCV therapy represent a highly promising area for the discovery of prognostic and predictive factors. Therefore, the aim of our study was to develop autologous cellular models that reproduce *in vitro* the activation of antitumor mechanisms resulting from exposure to DCV, and to investigate their prognostic value during treatment.

Materials and Methods

Patient Material Characteristics

This study included biological samples from 11 patients: 7 with disseminated forms of cutaneous melanoma (CM) and 4 with soft tissue and osteogenic sarcomas (STS/OS), all of whom received autologous dendritic cell vaccination (DCV, CaTeVac) at the N.N. Petrov National Medical Research Center of Oncology, Ministry of Health of Russia [7]. The study protocol was approved by the Institutional Ethics Committee, and written informed consent was obtained from all participants. Detailed clinical characteristics of the patients are presented in Table 1. Among STS/OS patients, 2 had osteogenic sarcoma, 1 had pleomorphic rhabdomyosarcoma, and 1 had a tumor of the peripheral nerve sheath. For analysis of differential clinical effects of DCV, patients were stratified based on therapeutic response as having a sufficient effect (SE) or an insufficient effect (IE). Sufficient effect was defined as the absence of disease progression for at least 6 months under standalone (palliative) therapy or 12 months with adjuvant immunotherapy [8]. Six patients experienced SE and received 12–62 DCV cycles, while five showed IE with 4–12 DCV cycles.

Table 1. Patient Characteristics

Patient Characteristic		CM	STS/OS
N		7	4
Age, years	Median	52	19.5
	Range	21–65	18–33
Sex	Male	3	4
	Female	4	0
Disease stage	II	0	0
	III	6	0
	IV	1	4
Previous lines of systemic treatment	0	7	0
	1	0	1
	2	0	1
	3 and more	0	2
DC therapy mode	Adjuvant	7	1
	Therapeutic	0	3
No of DC therapy cycles	Median	12	19
	Range	4–62	6–23
Effect of DC therapy	SE	3	3
	IE	4	1

CM — cutaneous melanoma; STS/OS — soft tissue sarcomas and osteogenic sarcomas; SE — Sufficient effect; IE — Insufficient effect.

Isolation and Cultivation of Malignant Tumor Cells

Tumor tissue fragments were mechanically dissociated using a Medimachine (Agilent Technologies, USA). Tumor cells were seeded into plastic culture flasks (Sarstedt, Germany) and continuously cultured in a CO_2 incubator ("Heracel", Thermo Electron LTD GmbH, Germany) according to Freshney's protocols [9] with in-house modifications [10], using DMEM/F12 medium (Biolot, Russia) supplemented with 20 % fetal bovine serum (Biolot, Russia), 20 % conditioned medium from human embryonic lung fibroblasts, insulin (5 μg/mL), transferrin (5 μg/mL), and selenium (5 ng/mL) (Invitrogen, USA). Upon reaching confluence, subculturing was performed using equal volumes of 0.25 % trypsin and 0.02 % versene (Biolot, Russia). Continuous culturing of tumor cells was maintained for a minimum of 10 passages, where each passage denotes a single round of cell seeding and growth in culture [9]. Real-time monitoring of tumor cell growth was performed using a Cell-IQ system (Chip Man Technologies, Finland).

To prevent fibroblast contamination, geneticin was added at a concentration of 100μg/mL [11]. Culture purity was controlled using flow cytometry (FACS Canto II, BD, USA) with monoclonal antibodies targeting the fibroblast marker ER-TR7 (Santa Cruz Biotech, USA).

Cultivation of Dendritic Cells

For generation of autologous vaccine DCs, the adherent CD14+ monocyte fraction was isolated from the peripheral blood of oncology patients and processed using a previously optimized protocol [7]. Differentiation was performed in balanced serum-free "Cell-Gro DC" medium (CellGenix, Germany) in high-adhesion culture flasks (TPP, Switzerland) at 37 °C, 5 % CO_2, and 98 % humidity. Granulocyte-macrophage colony-stimulating factor (GM-CSF, 72ng/mL) and interleukin-4 (IL-4, 20 ng/mL) (CellGenix, Germany) were added on days 1, 3, and 5 of cultivation. For antigen loading and specific activation, on day 7, immature DCs ($CD14\text{-}CD1a^{+}$) were pulsed with IRTAN-2018, a lysate cocktail of nine allogenic HLA-positive tumor cell lines [12], and exposed to lysed tumor cells at a 3:1 ratio. Tumor necrosis factor-alpha (TNF-α, 20 ng/mL), IL-4 (20 ng/mL), and GM-CSF (72 ng/mL) were added simultaneously. After 48 hours, DCs with the phenotype $CD1a^{-}CD83^{+}$ were harvested by centrifugation.

At all stages, DCs were assessed for lineage and differentiation antigen expression using laser flow cytometry (BD FACSCanto II, BD, USA) with fluorochrome-conjugated monoclonal antibodies: CD14-FITC, CD1a-APC, CD83-PE-Cy7, CD80-APC-Cy7, CD86-PerCP-Cy5.5, CD40-PE, HLA-DR-APC-Cy7, CD209-PerCP-Cy5.5, and CCR7-BV421[13].

Cultivation of Activated Lymphocytes

Lymphocytes were activated by co-culturing with autologous vaccine DCs. Cryopreserved lymphocyte suspensions were thawed and introduced into the culture system. On day 16, the lymphocyte fraction was collected and transferred to a new culture system with fresh DCs loaded with tumor antigens. Continuous co-culture with DCs and lymphocytes was carried out for 14 days in the presence of cytokines IL-2 (12.5 IU/mL) and IL-7 (10 ng/mL).

Assessment of Induced T-Cell Proliferation

Induced T-cell proliferation was assessed using the fluorescent dye CFSE (5μM). Vaccine DCs were added at an effector:target ratio of 10 : 1 to induce effector T-cell proliferation. The relative content of proliferating T cells was evaluated on day 5 of co-culture by tracking CFSE dilution using flow cytometry (FACS Canto II, BD Biosciences, USA) and BD FACSDiva software (version 8.0.1). Spontaneous proliferation of CFSE-labeled lymphocytes served as a negative control.

Analysis of the Pool Composition of Proliferating T Lymphocytes Activated in vitro

The subpopulation structure of proliferating T cells induced by mature DCs was analyzed by flow cytometry (FACS Canto II, BD Biosciences, USA) using monoclonal antibodies conjugated with fluorochromes: CD45RA-PE, CD28-PerCP-Cy5.5, CD8-PE-Cy7, CD3-APC, CD45-APC-Cy7, and CD197-BV421 (CCR7) (BD Biosciences, USA) and the BD FACSDiva program (version 8.0.1). Antigen-specific granzyme B (GrB) production by T cells was assessed by intracellular staining with monoclonal antibodies using specific protocols for fixation and membrane permeabilization (BD Cytofix/Cytoperm™).

Cytotoxicity Assay

Cytotoxicity was evaluated by analyzing proliferation of malignant tumor cells co-cultured with specifically activated T-lymphocytes using the xCELLigence RTCA DP Instrument (ACEA Biosciences, USA). Tumor cells (2×10^4/well) were seeded into E-Plate View 96-well plates (ACEA Biosciences, USA). After 24 hours, autologous activated T-lymphocytes were added at an effector: target ratio of 10:1 and incubated for 48 hours. Tumor cell cultures without effectors served as controls. Cell lysis was assessed by calculating the Slope parameter associated with the rate of change of cell index, reflecting the number of viable adherent cells. The cell lysis coefficient (CL) was calculated as follows:

$$(CL) = \frac{Slope_{contrl} - Slope_{exp}}{Slope_{exp.}} \times 100\ \%$$

Creation of Three-Dimensional Cellular Constructs (Spheroids)

Tumor spheroids were generated using low-adhesion surface technology with 96-well Ultra-Low Attachment Surface (Corning, USA). Patient-derived tumor cells were inoculated into plate wells in quantities of 1–2×10⁴ in 200μL of complete medium and cultivated for 3–8 days in a CO_2 incubator, "Heracel" (Thermo Electron LTD GmbH, Germany) at 37°C, 100 % humidity, and 5 % CO_2. Activated T-lymphocytes, pre-stained with CFSE (5μM), were added at a ratio of 1 tumor cell: 20 lymphocytes and incubated for 3–5 days. Cell interactions were monitored in real time with the Cell-IQ system (Chip Man Technologies, Finland). Spheroid cell viability was assessed by flow cytometry using the viability dye 7AAD.

Analysis of Immunosuppressive Factor Production

Levels of immunosuppressive factors (ISFs) — transforming growth factor β1 (TGFβ1), interleukins IL-6, IL-8, and IL-10 — were quantified in tumor cell supernatants and patient serum using multiplex analysis (BioPlex® 200, Bio-Rad, USA) and Bio-Plex Manager™ v6.1 software. The NK-G2D ligand MICA levels were determined with the MICA Duoset ELISA Kit (R&D Systems, USA).

To model a suppressive tumor microenvironment, MICA (100 pg/mL), $TGFβ_1$ (30 pg/mL), IL-6 (25 pg/mL), IL-8 (50 pg/mL), and IL-10 (50 pg/mL) were added to the experimental cell system.

Statistical Analysis

Data analysis was performed using IBM SPSS 19.0 and Microsoft Excel 2010. Descriptive statistics, correlation analysis, and nonparametric testing (Spearman and Mann–Whitney criteria) were applied for analysis of differences between independent groups [14].

Results

Assessment of *in vitro* induced T-cell proliferation demonstrated that, in 90.9 % of patients (10 out of 11), activated T lymphocytes were generated in response to stimulation by vaccine-derived DCs prior to the start of DCV therapy. Furthermore, with an increasing number of immunotherapy cycles, the percentage of proliferating T cells continued to rise (Table 2, online application). However, in patients with an IE, after each cycle of DC vaccination, the $CD3^+CFSE^+$ lymphocyte population was quantitatively lower compared to patients with a SE (Fig. 1).

Modeling the interaction of activated T lymphocytes — generated via co-cultivation with mature DCs corresponding to specific vaccination cycles — with autologous malignant tumor cells reproduced real clinical outcomes in 8 of 11 (72.7 %) cases (Table 3, online application). Fig. 2 shows the results of cellular model studies using biological material from patients with cutaneous melanoma who developed either SE or IE. In patient ISA with SE, an increase in the number of proliferative $CD3^+CFSE^+$ lymphocytes during DC therapy was accompanied by enhanced cytotoxic properties, resulting in complete suppression of the growth of melanoma cell culture #1111, as measured by the xCELLigence analyzer, with the Slope value dropping to negative numbers (Fig. 2. А1, А2, А3). In patient SHUR, who failed to achieve SE after 12 cycles of DC therapy, an increase in proliferating $CD3^+CFSE^+$ lymphocytes was also observed, but no effective lysis of autologous target tumor cells occurred. This was indicated by a comparison of growth rates of melanoma cell culture #912 in the presence and absence of lymphocytes (Fig. 2. Б1, Б2, Б3). Similar results were obtained for STS/OS patients: those with IE exhibited markedly reduced

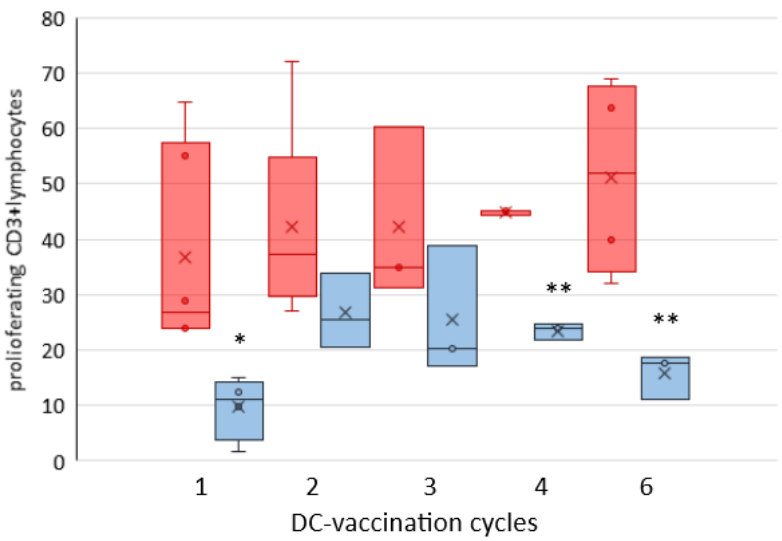

Fig. 1. Generation of activated T-lymphocytes in response to stimulation by vaccine DCs in patients with SE and IE. ■ — SE (Sufficient Effect); ■ — IE (Insufficient Effect). * Statistically significant differences (*p* = 0.038). ** Statistically significant differences (*p* = 0.050)

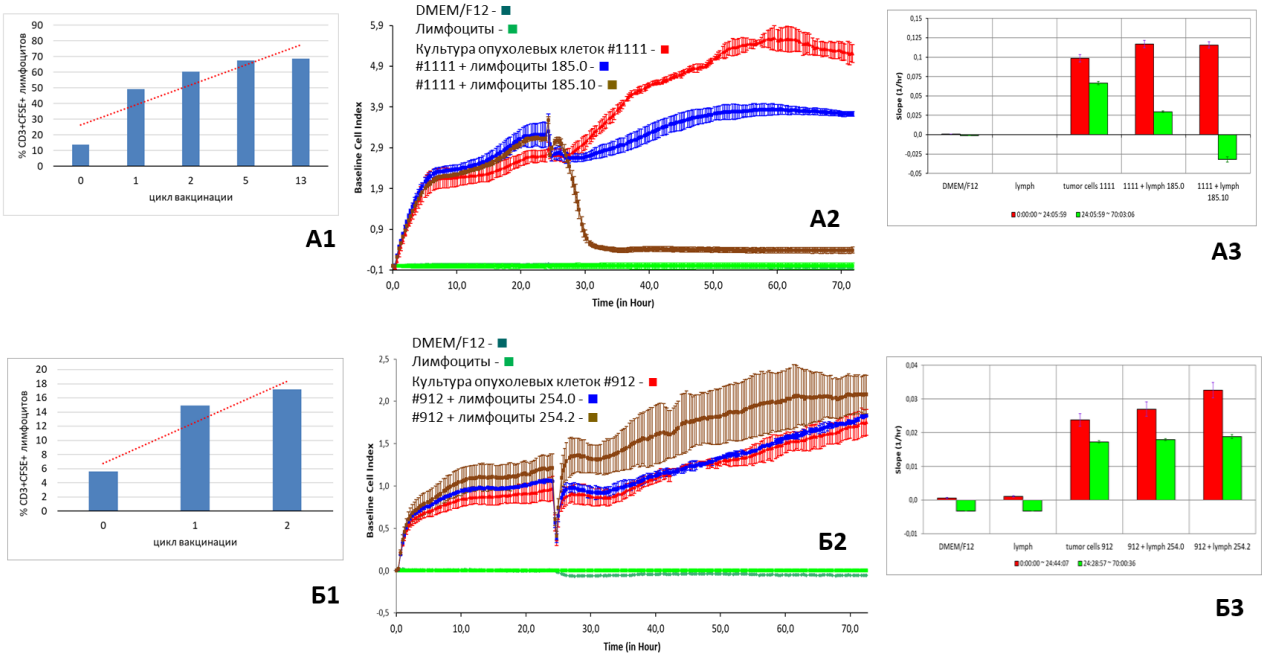

Fig. 2. Individual autologous cellular models for evaluating the efficacy of immunological synapses during DCV therapy in cutaneous melanoma (CM) patients. A: Patient ISA, 52 y.o., cutaneous melanoma, SE, 62 vaccination cycles. Б: Patient SHUR, 29 y.o., cutaneous melanoma, IE, 12 vaccination cycles. 1 — Dynamics of proliferating $CD3^{+}CFSE^{+}$ lymphocyte counts during co-culturing with vaccine DCs throughout DCV therapy. 2 — Proliferative activity of CM cells in a mixed culture with activated autologous T-lymphocytes. 3 — CM cell culture growth rate assessed via the *Slope* parameter using the xCELLigence cell analyzer.
А2, Б2: ■ — DMEM/F12, ■ — Lymphocytes, ■ — CM cell cultures #1111 and #912 (untreated control), ■ — Co-culture of CM cells and lymphocytes derived from PBMCs before vaccination, ■ — Co-culture of CM cells and lymphocytes derived from PBMCs during vaccination

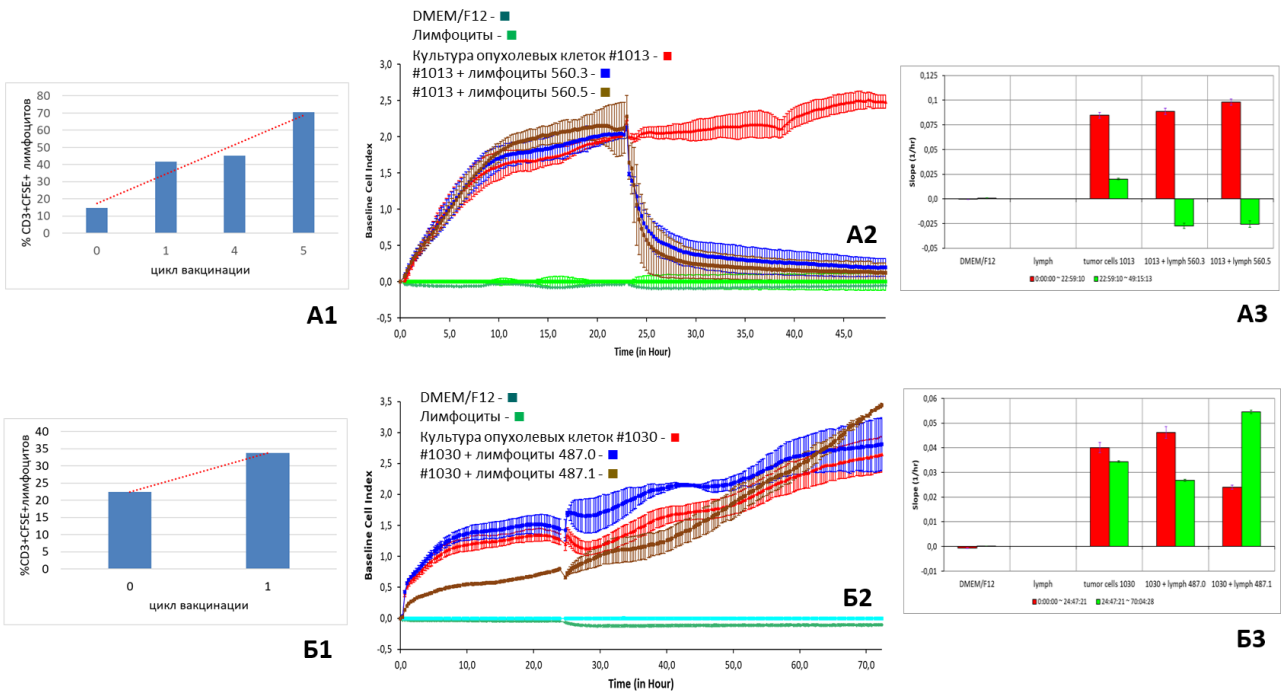

Fig. 3. Individual autologous cellular models for evaluating immunological synapse efficacy during DCV therapy in STS/OS patients. A: Patient DSA, 33 y.o., pleomorphic rhabdomyosarcoma (PRMS), SE, 23 vaccination cycles. Б: Patient OMS, 21 y.o., osteogenic sarcoma (OS), IE, 6 vaccination cycles. 1 — Dynamics of proliferating $CD3^{+}CFSE^{+}$ lymphocyte counts during co-culture with vaccine DCs throughout DCV therapy. 2 — Proliferative activity of STS/OS cells in mixed culture with activated autologous T-lymphocytes. 3 — STS/OS cell culture growth rate assessed via the *Slope* parameter using the xCELLigence cell analyzer.
А2, Б2: — ■ — DMEM/F12, ■ — Lymphocytes, ■ — Untreated control cultures (PRMS #1013 and OS #1030), ■ — Co-culture of STS/OS cells with lymphocytes derived from pre-vaccination PBMCs, ■ — Co-culture of STS/OS cells with lymphocytes derived from PBMCs during vaccination

reactivity of specifically activated T lymphocytes generated in the presence of vaccine DCs, resulting in continued tumor cell proliferation without cell death (Fig. 3).

A correlation was found between the parameters of the specific activity of T lymphocytes — generated from peripheral blood cells pre-treatment — and the production of ISFs by cultured tumor cells of the patients. A strong inverse correlation was observed between the content of MICA secreted by malignant cells and the CL (rho = –0.792, p = 0.001). A moderate inverse correlation was also found for $TGF\beta_1$ and CL (rho = –0.472, p = 0.048).

The number of proliferating, activated $CD3^+CFSE^+$ lymphocytes correlated with the quantitative content of ISFs in the patients' peripheral blood at the "zero time point" prior to vaccination. A moderate inverse correlation was observed between the relative content of $CD3^+CFSE^+$ lymphocytes after stimulation with activated DCs and the concentrations of IL-10 (rho = –0.579, p = 0.019)

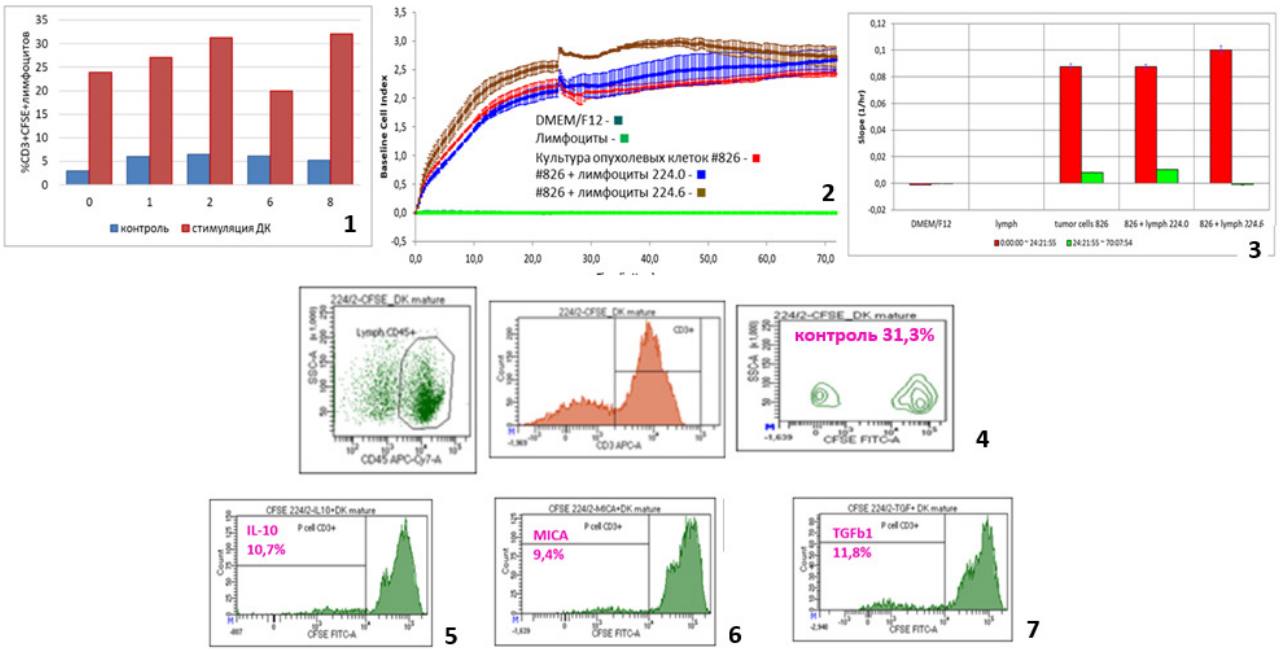

Fig. 4. Autologous cellular model using biological material from patient BVN, 36 y.o., cutaneous melanoma, receiving adjuvant DC therapy (20 cycles). 1 — Evaluation of proliferating $CD3^+CFSE^+$ lymphocyte populations generated in response to stimulation by vaccine DCs during therapy. Spontaneous T-lymphocyte proliferation was assessed as control; 2 — Dynamics of the cell index, reflecting proliferative activity of tumor cells in mixed culture with activated autologous T-lymphocytes; 3 — Growth rate assessment of cutaneous melanoma cell culture #826 via the *Slope* parameter using the xCELLigence cell analyzer; 4 — Quantitative analysis of proliferating $CD3^+CFSE^+$ lymphocytes (31.3 %) by flow cytometry after 2 cycles of DC therapy; 5 — Quantitative analysis of proliferating $CD3^+CFSE^+$ lymphocytes (10.7 %) by flow cytometry after 2 cycles of DC therapy in the presence of IL-10; 6 — 9.4 % in the presence of MICA; 7 — 11.8 % in the presence of $TGF\beta_1$

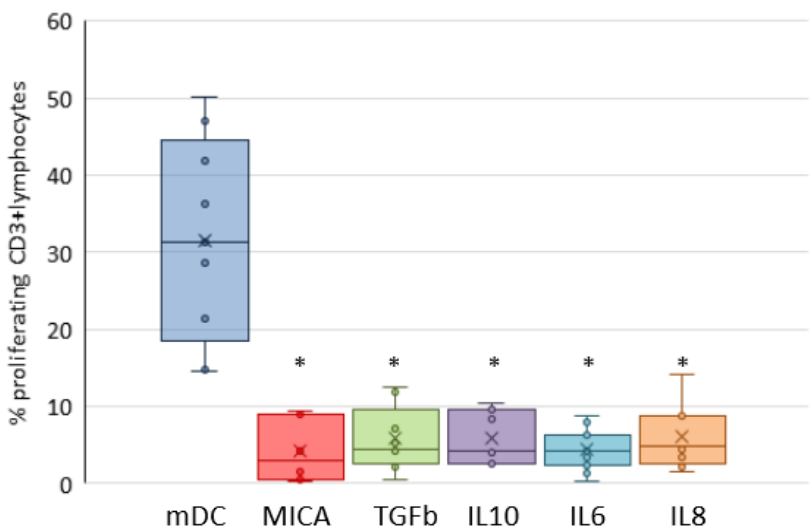

Fig. 5. Modeling the effects of ISF on activated T-lymphocyte clone formation: mDC: Intact system with mature DC co-culture, MICA: NKG2D receptor ligand, TGFb: With transforming growth factor β1, IL-10: Interleukin 10, IL-6: Interleukin 6, IL-8: Interleukin 8. Vaccine DCs were derived from peripheral blood monocytes after 2-6 DCV cycles (n=13). * - Statistically significant differences (p<0.05)

and TGFβ$_1$ (rho = –0.512, p = 0.043) in pre-treatment peripheral blood.

During T-cell activation, a statistically significant increase was found in the proportion of terminally differentiated effector memory T cells (TEMRA) for both CD4$^+$ (p = 0.018) and CD8$^+$ (p = 0.048) subsets in SE patients prior to DC therapy versus those with IE. In the modeling of cell interactions after 2–6 cycles of DCV, SE patients showed a significant rise in CD8$^+$ effector memory T cells (CD8$^+$Tem) (p = 0.036) and in TEMRA CD8$^+$ lymphocytes producing granzyme B (TEMRA GrB$^+$CD8$^+$) (p = 0.025).

A more detailed study of cellular models that did not mirror the real clinical situation demonstrated the critical role of immunosuppressive tumor microenvironment components — such as ISFs — in modulating the function of activated immune cells, and highlighted the necessity for careful selection of prognostic cellular model components. Fig. 4 presents analysis results from a cellular model derived from patient BVN, 36 years old, with cutaneous

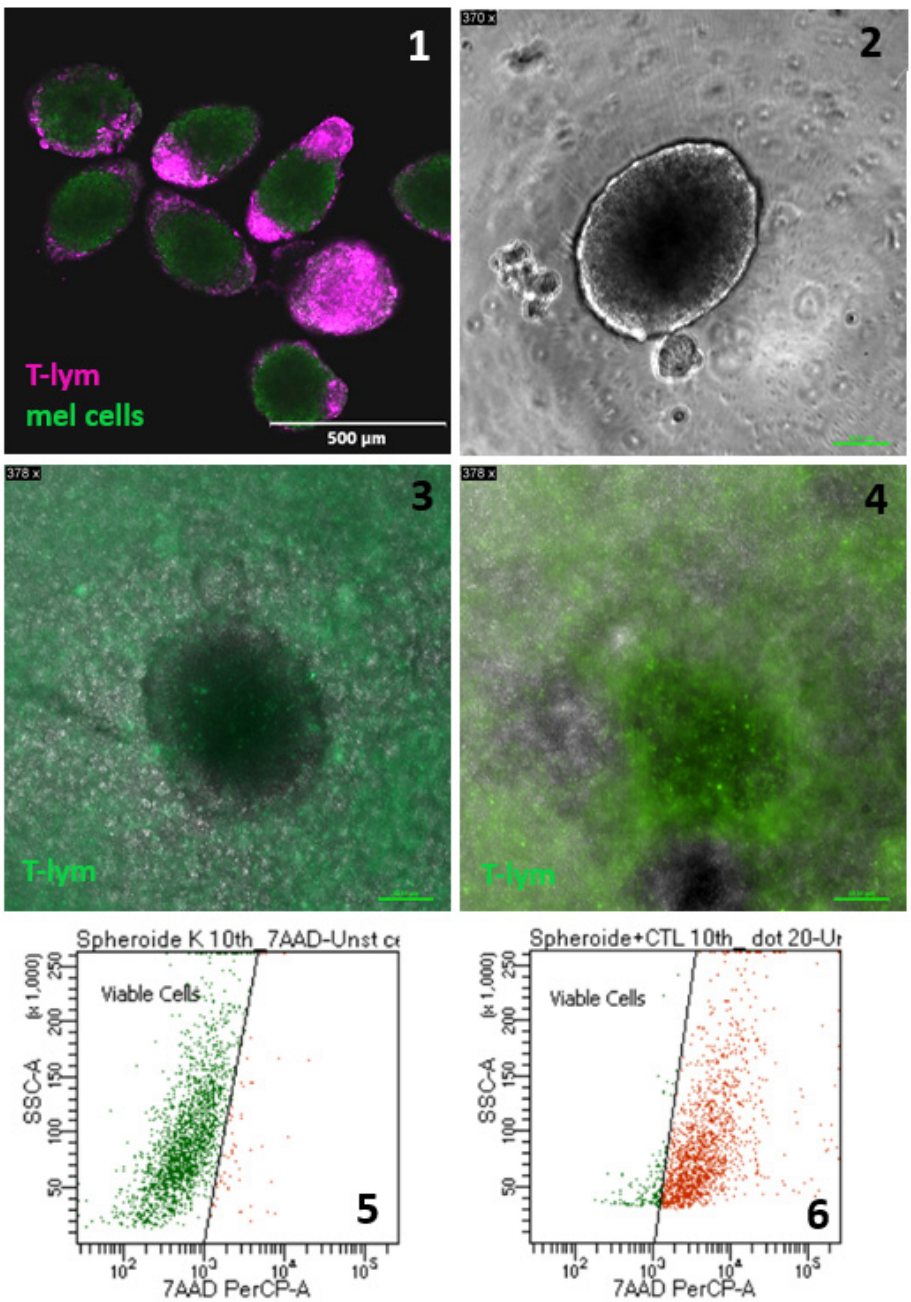

Fig. 6. Interaction between activated T-lymphocytes and tumor cells in 3D cellular models: 1 — Melanoma cell spheroids (#1111 from patient I.) after 24-hour incubation with activated CFSE$^+$CD3$^+$ lymphocytes. T-lymphocytes localize in the cortical zone of spheroids. Confocal microscopy, scale bar: 500 µm; 2 — Intact melanoma spheroid (#1111), phase contrast (Cell-IQ), scale bar: 32.51 µm; 3 — Co-culture of CFSE$^+$CD3$^+$ lymphocytes with spheroid #1111, day 1. Combined phase-contrast and fluorescence imaging (Cell-IQ), scale bar: 32.51 µm; 4 — Spheroid #1111 destruction by activated T-lymphocytes on day 8. Combined phase-contrast and fluorescence imaging (Cell-IQ), scale bar: 32.51 µm; 5 — Viability assessment of intact spheroid #1111 by flow cytometry: 97.4 % viable cells; 6 — Viability assessment of spheroid #1111 after incubation with activated T-lymphocytes (20 DCV cycles) by flow cytometry: 8.9 % viable cells

melanoma, who received 20 cycles of DCV with SE. Assessment of the proliferating $CD3^+CFSE^+$ lymphocyte population generated in response to DC stimulation showed positive dynamics during therapy (Fig. 4–1). However, in this model, there was no difference in the growth rate between intact melanoma cell culture #826 and culture co-cultivated with specifically activated T lymphocytes (derived from peripheral blood mononuclear cells obtained before vaccination and after the 6th DCV cycle) (Fig. 4–2, –3). It was revealed that adding ISFs to the experimental co-culture system of autologous activated DCs and lymphocytes reduced the $CD3^+CFSE^+$ lymphocyte population nearly threefold (Fig. 4–4, –5, –6, –7). The relative content of $CD3^+CFSE^+$ lymphocytes after 2 DCV cycles was 31.3 % (by flow cytometry). Addition of IL-10 to the co-culture medium reduced this to 10.7 %, MICA to 9.4 %, and $TGF\beta_1$ to 11.8 %. Enzyme immunoassay of ISF concentrations in the supernatant from melanoma culture #826 (at passage 106), showed high levels of MICA (5,237.8 pg/mL), $TGF\beta_1$ (18.9 ng/mL), IL-10 (176.0 pg/mL), and VEGF (1,022.5 pg/mL) compared to control fibroblast culture FLECH. After this model was characterized, immunosuppressive conditions were replicated in experiments with cells from other patients, yielding similar results (Fig. 5). Statistically significant differences were found in the proportion of proliferating T lymphocytes forming clones after multiple DCV cycles, both with and without exposure to ISFs (MICA, $TGF\beta_1$, IL-6, IL-8, IL-10) ($p < 0.05$).

The effectiveness of tumor cell lysis by activated T lymphocytes was studied in autologous 3D models using cultures of melanoma and various types of sarcomas. After the formation of tumor spheroids, autologous activated $CD3^+CFSE^+$ lymphocytes were added to experimental systems for real-time monitoring of cell interactions; tumor cell viability and lymphocyte tumor infiltration were assessed with flow cytometry. After one day of co-culture, $CD3^+$ lymphocytes localized to the cortical zone of spheroids (Fig. 6-1); by day 3, they accounted for 26–30 % of all cells. In the presence of T lymphocytes, spheroid structure was disrupted, with compact, sharply contoured formations in intact systems and at early co-culture stages being lost (Fig. 6–2, 3). By day 8, complete spheroid destruction was observed, and the proportion of dead cells exceeded 90 % (Fig. 6–4, 5, 6).

Discussion

The antitumor efficacy observed with immune checkpoint inhibitors and CAR-T cell therapies has convincingly demonstrated the potential of the immune system to control malignancies. However, it has become clear that the effectiveness of these treatment modalities for malignant tumors is subject to notable limitations [15]. For instance, the success of immune checkpoint inhibitors is often contingent upon significant infiltration of cytotoxic T lymphocytes within the tumor microenvironment — a parameter lacking in a substantial proportion of patients [16]. In contrast, therapeutic anticancer cellular vaccines represent an active immunization strategy aimed at stimulating adaptive immune responses against tumor antigens, ultimately generating tumor-specific functional immune effectors, including cytotoxic T lymphocytes. The rationale for utilizing DC-based vaccines loaded with tumor antigens is robustly grounded in their capacity to potentiate natural immune processes [17].

In vitro modeling and the study of cellular interactions induced by such vaccines have proven to be valuable tools for monitoring treatment and predicting clinical outcomes. In this article, we reported on the creation and analysis of autologous cellular models that replicate *in vitro* the functional activity of specifically activated T lymphocytes generated through co-culture with vaccine-induced DCs loaded with lysates from nine melanoma cell cultures, highly expressing cancer-testis antigens (IRTAN-2018). Previous studies revealed that interaction with such DCs can generate T lymphocytes capable of destroying not only melanoma cells but also other tumor types, with the efficiency of cell lysis correlating with the transcriptional activity of cancer-testis genes in target cells. [18].

We focused on establishing autologous cellular models that recapitulate *in vitro* the interaction between vaccine DCs and naïve T lymphocytes, leading to their specific activation, clonal expansion, and the lysis of patient tumor cells. In the *in vitro* system, almost all patients, regardless of DCV effectiveness, exhibited generation of activated T lymphocytes, and the magnitude of these populations correlated with therapeutic efficacy. We obtained mature DCs from monocytes isolated from patients' peripheral blood at various treatment stages, and observed that lymphocyte cytotoxicity increased with the number of DCV cycles. At the same time, the immunosuppressive tumor microenvironment — potentially shaped by the secretory activity of malignant cells capable of generating factors that block antitumor immune responses and/or polarize tumor-associated immune cells — was found to impact the intensity of activated $CD3^+$ cell generation and the killing capacity against tumor target cells in experimental systems.

It is important to note that the early stages of antitumor cellular immunotherapy highlighted the ability of DCVs to elicit antitumor immune responses; however, clinical trial results have often been limited by the effects of the immunosuppressive

tumor microenvironment [19]. We demonstrated that, within cellular models, the NKG2D receptor ligand MICA, the factor $TGF\beta_1$, and interleukins IL-6, IL-8, IL-10 led to approximately a threefold reduction in the pool of $CD3^+CFSE^+$ lymphocytes. Furthermore, the functional characteristics of vaccine-derived DCs generated from $CD14^+$ monocytes obtained from the peripheral blood of patients before treatment were associated with specific concentrations of IL-10 and $TGF\beta_1$ in circulation.

The functional activity of *in vitro* activated T lymphocytes differed significantly between patients with sufficient and insufficient DCV effects throughout therapy. This variance was also reflected in increased proportions of TEMRA GrB^+CD8^+ cells and $CD8^+$Tem in the experimental system upon achievement of SE. It is well established that priming naive $CD8^+$ T cells triggers clonal expansion and acquisition of tissue homing, effector function, and cytolytic activity. After the contraction of the effector T cell response, memory T cells continue to recirculate and may become tissue-resident throughout the body [20]. It is plausible that expansion of the Tem pool may be associated with SE of the treatment.

Three-dimensional models such as spheroids more accurately reflect the immunomodulatory, proliferative, and activation interactions characteristic of malignancies compared to two-dimensional cultures [21]. We conducted a series of experiments using spheroids derived from melanoma and various sarcoma cell types. Notably, in the three-dimensional system, activated T lymphocytes initially concentrate at the periphery of tumor spheroids, subsequently infiltrate the cortical zone, and ultimately distribute diffusely throughout the spheroid — regardless of spheroid histological type. Under the influence of lymphocytes, spheroids lose structural integrity and fragment into elements composed of over 90 % dead cells positive for 7-AAD dye. Comparable findings have been reported by other investigators using established tumor cell lines, including colorectal cancer [22]. Moreover, antibodies directed against specific NKG2D ligands MICA and MICB have been shown to enhance immune-mediated spheroid destruction by promoting increased infiltration and activation of NK cells within this system. In our experiments, the presence of MICA molecules markedly inhibited T lymphocyte activation, and the degree of spheroid destruction correlated with patient response to DCV therapy.

Conclusion

Experimental data demonstrate the cytotoxic capacity of antigen-specific T lymphocytes generated via induction with mature DCs against autologous tumor cells. The cytotoxic properties of activated lymphocytes differ among patients and reflect the clinical course of the disease and therapeutic response, thereby supporting the use of cellular modeling in both 2D and 3D formats as a valuable *in vitro* method for predicting and monitoring the efficacy of cell-based therapy.

Acknowledgments
The authors gratefully acknowledge N.A. Emelyanova, MD, clinical laboratory diagnostics, for her expert technical support in performing the flow cytometry analysis.

Conflict of Interest
The authors declare no conflicts of interest.

Funding
This research was conducted as part of a state-funded assignment: “Development of innovative autologous medicinal products based on somatic cells tailored to the individual immunogenetic profile of the patient for the treatment of aggressive malignant neoplasms”.

Compliance with patient rights and principles of bioethics
All procedures performed in studies involving human participants were in accordance with the ethical standards of Declaration of Helsinki Protocol (2013). The study protocol No 23/48, dated 20 February 2020 was approved by the Institutional Ethics Committee, and written informed consent was obtained from all participants.

Author Contributions
Nekhaeva T.L.: Conceptualization, experimental execution, and drafting of the original manuscript.
Danilova A.B.: Microscopic cytological analysis, generation of 3D cell models, analysis of tumor cell invasivity using the xCELLigence platform, and data interpretation.
Efremova N.A.: Patient selection, establishment of 2D/3D solid tumor cell cultures, and data interpretation.
Danilov A.O.: Flow cytometry, enzyme-linked immunosorbent assay (ELISA), statistical analysis, and data interpretation.
Zuy E.S.: Statistical analysis and data interpretation.
Baldueva I.A.: Critical analysis of the study, intellectual contribution, and critical revision of the manuscript.

REFERENCES

1. Swartz A.M., Hotchkiss K.M., Smita N.K., et al. Generation of tumor targeted dendritic cell vaccines with improved immunogenic and migratory phenotype. *Methods Mol Biol*. 2022: 2410: 609-626.-DOI: https://doi.org/10.1007/978-1-0716-1884-4_33.-URL: https://link.springer.com/protocol/10.1007/978-1-0716-1884-4_33.
2. Mastelic-Gavillet B., Balint K., Boudousquie C., et al. Personalized dendritic cell vaccines-recent breakthroughs and encouraging clinical results. *Front Immunol*. 2019; 10: 766.-DOI: https://doi.org/10.3389/fimmu.2019.00766.-URL: https://www.frontiersin.org/journals/immunology/articles/10.3389/fimmu.2019.00766/full.
3. Hato L., Vizcay A., Eguren I., et al. Dendritic cells in cancer immunology and immunotherapy. *Cancers* (Basel). 2024; 16(5): 981.-DOI: https://doi.org/10.3390/cancers16050981.--URL: https://www.mdpi.com/2072-6694/16/5/981.

4. Lurje I., Hammerich L., Tacke F. Dendritic cell and t cell crosstalk in liver fibrogenesis and hepatocarcinogenesis: implications for prevention and therapy of liver cancer. *Int J Mol Sci*. 2020; 21: 7378.-DOI: https://doi.org/10.3390/ijms21197378.-URL: https://www.mdpi.com/1422-0067/21/19/7378.
5. Lehmann B.D., Colaprico A., Silva T.C., et al. Multi-omics analysis identifies therapeutic vulnerabilities in triple-negative breast cancer subtypes. *Nat Commun*. 2021; 12: 6276.-DOI: https://doi.org/10.1038/s41467-021-26502-6.-URL: https://www.nature.com/articles/s41467-021-26502-6.
6. González F.E., Gleisner A., Falcón-Beas F., et al. Tumor cell lysates as immunogenic sources for cancer vaccine design. *Hum Vaccines Immunother*. 2014; 10: 3261–3269.-DOI: https://doi.org/10.4161/21645515.2014.982996.-URL: https://pmc.ncbi.nlm.nih.gov/articles/PMC4514089/.
7. Nekhaeva T.L. Optimization of autologous dendritic cell vaccines for the treatment of patients with malignant neoplasms. *Siberian Oncol J*. 2013; 57(3): 52–56 (In Rus).
8. Danilova A.B., Novik A.V., Nekhaeva T.L., Balduyeva I.A. The role of immunosuppressive factors in prognosis of the efficacy of cellular immunotherapy in patients with solid tumors. *Effective Pharmacother*. 2022; 18(17): 8–17.-DOI: https://doi.org/10.33978/2307-3586-2022-18-17-8-17.-URL: https://umedp.ru/upload/iblock/961/effektivnaya_farmakoterapiya_onkologiya_gematologiya_i_radiologiya_5_2022.pdf (In Rus).
9. Freshney R.I. Culture of animal cells: a manual of basic technique and specialised applications. 6th ed. Hoboken, NJ: Wiley-Blackwell. 2010; 732.
10. Danilov A.O., Larin S.S., Danilova A.B., et al. Optimization of a method for the preparation of vaccines based on autologous genetically modified tumor cells for the treatment of patients with disseminated cutaneous melanoma. *Russ Biother J*. 2003; 2(3): 47-53 (In Rus).
11. Levin D.B., Wilson K., Valadares de Amorim G., et al. Detection of p53 mutations in benign and dysplastic nevi. *Cancer Research*. 1995; 55(19): 4278–4282.
12. Patent 2714208 C1. Balduyeva I.A, Danilova A.B., Nekhaeva T.L., Avdonkina N.A., Emelyanova N.V., Belyaev A.M. Cell product for loading and activation of human dendritic cells. Russian Federation: Federal State Budgetary Institution “National Medical Research Center of Oncology named after N.N. Petrov” of the Ministry of Health of the Russian Federation. Priority date 2019.03.05. 2020. Bull. No. 5 (In Rus).
13. Nekhaeva T.L., Balduyeva I.A., Novik A.V., et al. Development and optimization of vaccines based on autologous dendritic cells activated by cancer–testis antigens for the treatment of cutaneous melanoma. *Bull Ural Med Acad Sci*. 2014; (5): 92–98 (In Rus).
14. Everitt B.S., Pickles A. Statistical aspects of the design and analysis of clinical trials. Imperial College Press. London. 2004.
15. Tiwari A., Alcover K., Carpenter E., et al. Utility of cell-based vaccines as cancer therapy: Systematic review and meta-analysis. *Hum Vaccin Immunother*. 2024; 20(1): 2323256.-DOI: https://doi.org/10.1080/21645515.2024.2323256.-URL: https://pmc.ncbi.nlm.nih.gov/articles/PMC10984131/.
16. Gide T.N., Wilmott J.S., Scolyer R.A., Long G.V. Primary and acquired resistance to immune checkpoint inhibitors in metastatic melanoma. *Clin Cancer Res*. 2018; 24(6):1260–1270.-DOI: https://doi.org/10.1158/1078-0432.CCR-17-2267.-URL: https://aacrjournals.org/clincancerres/article/24/6/1260/468/Primary-and-Acquired-Resistance-to-Immune.
17. Sellars M.C., Wu C.J., Fritsch E.F. Cancer vaccines: building a bridge over troubled waters. *Cell*. 2022; 185(15): 2770–2788.-DOI: https://doi.org/10.1016/j.cell.2022.06.035.--URL: https://www.cell.com/cell/fulltext/S0092-8674(22)00787-5?_return.-URL = https %3A %2F %2Flinkinghub.elsevier.com %2Fretrieve %2Fpii %2FS0092867422007875 %3Fshowall %3Dtrue.
18. Danilova A., Misyurin V., Novik A. et al. Cancer/testis antigens expression during cultivation of melanoma and soft tissue sarcoma cells. *Clin Sarcoma Res*. 2020; 10(3).-DOI: https://doi.org/10.1186/s13569-020-0125-2.-URL: https://clinicalsarcomaresearch.biomedcentral.com/articles/10.1186/s13569-020-0125-2.
19. Borges F., Laureano R.S., Vanmeerbeek I., et al. Trial watch: anticancer vaccination with dendritic cells. *Oncoimmunology*. 2024; 13(1): 2412876.-DOI: https://doi.org/10.1080/2162402X.2024.2412876.-URL: https://pmc.ncbi.nlm.nih.gov/articles/PMC11469433/.
20. Han J., Khatwani N., Searles T.G., et al. Memory CD8(+) T cell responses to cancer. *Semin Immunol*. 2020; 49: 101435.-DOI: https://doi.org/10.1016/j.smim.2020.101435.-URL: https://pmc.ncbi.nlm.nih.gov/articles/PMC7738415/.
21. Boucherit N., Gorvel L., Olive D. 3D tumor models and their use for the testing of immunotherapies. *Front Immunol*. 2020; 11: 603640.-DOI: https://doi.org/10.3389/fimmu.2020.603640.-URL: https://www.frontiersin.org/journals/immunology/articles/10.3389/fimmu.2020.603640/full.
22. Courau T., Bonnereau J., Chicoteau J., et al. Cocultures of human colorectal tumor spheroids with immune cells reveal the therapeutic potential of MICA/B and NKG2A targeting for cancer treatment. *J Immunother Cancer*. 2019; 7(1): 74.-DOI: https://doi.org/10.1186/s40425-019-0553-9.-URL: https://jitc.biomedcentral.com/articles/10.1186/s40425-019-0553-9.

Received / 24.09.2025
Reviewed / 26.10.2025
Accepted for publication / 18.12.2025

Author Information / ORCID

Tatyana L. Nekhaeva / ORCID ID: https://orcid.org/0000-0002-7826-4861; eLibrarySPIN: 5366-8969; Researcher ID (WOS): L-7268-2018; Author ID (Scopus):55317526900.

Anna B. Danilova / ORCID ID: https://orcid.org/0000-0003-4796-0386; eLibrary SPIN-9387-8328; Researcher ID H-7828-2014; Author ID 7005563064.

Natalya A. Efremova / ORCID ID: https://orcid.org/0000-0002-3533-2721; eLibrarySPIN: 7352-9350; Researcher ID (WOS): P-3886-2015; Author ID (Scopus): 57194491563.

Aleksei O. Danilov / ORCID ID: https://orcid.org/0009-0004-2890-1246; eLibrarySPIN 3587-5413; Author ID (Scopus): 7203049937.

Ekaterina S. Zuy / ORCID ID: https://orcid.org/0009-0005-0672-5090; eLibrarySPIN 1817-1177; Researcher ID (WOS) OJU-1349-2025; Author ID (Scopus): 57817751600.

Irina A. Baldueva / ORCID ID: https://orcid.org/0000-0002-7472-4613; eLibrarySPIN: 7512-8789; Researcher ID (WOS): H-9574-2014; Author ID (Scopus):6602224742.